Original Article
A tumor vessel-targeting fusion protein elicits a chemotherapeutic bystander effect in pancreatic ductal adenocarcinoma

Chun-Te Chen[1], Yi-Chun Chen[1], Yi Du[1], Zhenbo Han[1], Haoqiang Ying[1,2,4], Richard R Bouchard[3,4], Jennifer L Hsu[1,5,6], Jung-Mao Hsu[1], Trevor M Mitcham[3], Mei-Kuang Chen[1,4], Hui-Lung Sun[1], Shih-Shin Chang[1,4], Donghui Li[7], Ping Chang[7], Ronald A DePinho[2,4], Mien-Chie Hung[1,4,5,6]

Departments of [1]Molecular and Cellular Oncology, [2]Cancer Biology, [3]Imaging Physics, [7]Gastrointestinal Medical Oncology, The University of Texas MD Anderson Cancer Center, Houston, Texas 77030, USA; [4]Graduate School of Biomedical Sciences, The University of Texas Houston Health Science Center, Houston, Texas 77030, USA; [5]Center for Molecular Medicine and Graduate Institute of Cancer Biology, China Medical University, Taichung 404, Taiwan; [6]Department of Biotechnology, Asia University, Taichung 413, Taiwan

Abstract: Pancreatic ductal adenocarcinoma (PDAC) is a highly lethal disease characterized by a prominent desmoplastic stroma that may constrain tumor progression but also limit the access of therapeutic drugs. In this study, we explored a tumor-targeting strategy that enlists an engineered anti-angiogenic protein consisting of endostatin and cytosine deaminase linked to uracil phosphoribosyltransferase (EndoCD). This protein selectively binds to tumor vessels to compromise tumor angiogenesis and converts the non-toxic 5-fluorocytosine (5-FC) to the cytotoxic 5-fluorouracil to produce a chemotherapeutic bystander effect at the pancreatic tumor site. We found that resveratrol increased the protein stability of EndoCD through suppression of chymotrypsin-like proteinase activity and synergistically enhances EndoCD-mediated 5-FC-induced cell killing. In various PDAC mouse models, the EndoCD/5-FC/resveratrol regimen decreased intratumoral vascular density and stroma formation and enhances apoptosis in tumors cells as well as in surrounding endothelial, pancreatic stellate, and immune cells, leading to reduced tumor growth and extended survival. Thus, the EndoCD/5-FC/resveratrol combination may be an effective treatment option for PDAC.

Keywords: PDAC, EndoCD, resveratrol, two photon, MRI, ultrasound

Introduction

Pancreatic ductal adenocarcinoma (PDAC) is the fourth leading cause of cancer-related death in the United States, with a 5-year survival rate of less than 6% [1, 2]. PDAC oncogenomics is characterized by oncogenic mutations of *Kras* and loss of the p53, SMAD4, and p16/CDKN2A tumor suppressors [3, 4]. In the case of *Kras*, while genetic extinction causes tumor regression [5], there are no effective therapeutic strategies targeting *Kras* or its signaling surrogates [6]. Moreover, the dense desmoplastic stroma of PDAC has been proposed to promote tumor development and drug resistance [2, 7, 8]. Some reports demonstrated that genetic depletion of stromal elements leads to more aggressive PDAC with a poorer survival rate [9, 10]. While the presence of stroma appears to have both positive and negative effects on PDAC development, depending on specific functional assays, it is clear that the stroma acts as a protective barrier for PDAC against therapeutic drugs in the tumor microenvironment. Therefore, strategies that disrupt this stromal fortress while simultaneously increasing the delivery of cancer-cell-killing drugs could result in an overall clinical benefit.

In this study, we investigated a strategy involving endostatin in combination with cytosine deaminase. Endostatin is an angiogenesis inhibitor that targets proliferating endothelial cells [11]. Multiple clinical trials of endostatin demonstrated a favorable safety profile but a lack of clinical benefit, thought to be due to the

protein's short half-life [12]. Cytosine deaminase linked to uracil phosphoribosyltransferase (CD) converts the prodrug 5-flucytosine (5-FC) to the chemotherapeutic drug 5-fluorouracil (5-FU) and has a greater cancer-cell-killing effect than cytosine deaminase alone. However, CD has a narrow therapeutic window, as it does not specifically target tumors [13, 14]. Previously, our laboratory demonstrated that an endostatin-CD (EndoCD) fusion protein effectively reduced tumor growth in mouse models of breast and colorectal cancers [15]. Administration of EndoCD via intravenous delivery in tumor-bearing mice converted the non-toxic 5-FC to the cytotoxic 5-FU, which accumulated at the tumor site with a concentration 70-fold higher than the clinically equivalent dose. These findings indicated that EndoCD/5-FC can both inhibit angiogenesis and chemotherapeutically target tumors and that this targeting may induce a bystander-killing effect on endothelial and tumor cells surrounding the vessels [15]. In view of the PDAC stroma-associated impediment to drug delivery, the potential of targeting the tumor microenvironment prompted us to further investigate the therapeutic efficacy of EndoCD/5-FC in animal models of PDAC.

Here, we report that EndoCD/5-FC has potent therapeutic efficacy against PDAC. In addition, we discovered that resveratrol, a stilbene phytoalexin found in the skin of grapes [16], increases the protein stability of EndoCD by reducing the activity of chymotrypsin-like proteinase. Resveratrol is known to sensitize tumor cells to multiple chemotherapeutic agents, such as 5-FU, gemcitabine, paclitaxel, and cisplatin [17]. We found that the combination of EndoCD/5-FC and resveratrol had a synergistic antitumor effect. By using a noninvasive high-frequency ultrasound imaging technique, we further showed that this combination suppressed the formation of pancreatic stroma in various mouse models of PDAC, including *Kras* mutant PDAC. Our findings suggest that EndoCD/5-FC/resveratrol may be an ideal treatment strategy for PDAC and should be tested in clinical trials.

Materials and methods

Reagents

5-fluorocytosine (5-FC) and resveratrol were purchased from TCI America (Portland, OR) and doxycycline was purchased from Alfa Aesar (Ward Hill, MA).

Cell lines

Capan1, AsPC1/luc, and murine PanO2/luc pancreatic adenocarcinoma cell lines were maintained in Dulbecco's modified Eagle's (DMEM)/F12 medium supplemented with 10% fetal bovine serum (FBS). MP1070, a primary murine pancreatic cancer cell line was developed from $Kras^{G12D}p53^{L/+}$ conditional genomic modified mouse, was generated by Dr. Ronald DePinho's laboratory. AsPC1/luc, PanO2/luc, and MP1070/luc with stable luciferase expression were maintained in either G418 or puromycin selection. Cell lines were validated by short tandem repeats (STR) DNA fingerprinting by using the AmpFISTR Identifiler PCR Amplification Kit according to the manufacturer's instructions (Applied Biosystems; catalogue no. 4322288).

Recombinant protein purification

EndoCD protein was generated as previously described [15] and dialyzed in either Tris-HCl or phosphate buffered saline (PBS) solution.

Cell viability assay

Cell viability was evaluated by the tetrazolium dye [3-(4,5-dimethylthiazol-2-yl)-2,5-diphenyltetrazolium bromide (MTT) [15, 18]. Pancreatic cancer cells Capan1, AsPC1/luc, or panO2/luc cells were seeded (1×10^4 cells/well) in a 96-well plate. Different doses of resveratrol or EndoCD recombinant proteins with 200 μg/ml of 5-FC were added into each well. After 48 hr, MTT (3-(4,5-Dimethylthiazol-2-yl)-2,5-diphenyltetrazolium bromide) solution at 50 μl per well (2 mg/ml; Sigma) was added into the cell culture and incubated for 2 hr, followed by the addition of 100 μl of dimethyl sulfoxide (Sigma) to each well. Absorbance at 570 nm was measured immediately using a multi-well scanner (Labsystems, Helsinki, Finland). The effect of drug combination was determined by calculation of the combination indices (CI) in CompuSyn software. A CI value < 1 indicates a synergistic effect [19].

Protein stability assay and serum co-culture assay

For the ex vivo protein stability assay, EndoCD (12.5 μM) was added to mice sera with or with-

out resveratrol (100 µM) in a 37°C incubator, and at the indicated time point, proteins were subjected to SDS-PAGE for Western blot analysis. Protein bands were quantitated by normalization to the protein band density on day 0. Capan1, AsPC1/luc, or PanO2/luc pancreatic cancer cells were then subjected to 1/10 of the pre-incubated 5 days mixture, and cell viability was analyzed after treatment for 48 hr. For the in vivo protein stability assay, mice were administered 40 mg/kg resveratrol orally once a day for a week and 60 mg/kg EndoCD intravenously injected once. After the first protein treatment, sera were collected from mice in each group (mouse = 3) and set as the first initial time point. The levels of EndoCD protein in sera were detected by a human endostatin ELISA kit (abcam 100508) at the indicated time point.

Mouse treatment studies

For the orthotopic xenograft model, nude mice were inoculated with 1×10^6 AsPC1/luc human pancreatic cancer cells or MP1070/luc into the pancreas. Mice received 40 mg/kg resveratrol (five times per weeks) by oral injection [20] and/or 7.5 mg/kg EndoCD (twice per week) by tail-vein injection. For mice treated with EndoCD or EndoCD/resveratrol, 500 mg/kg 5-FC was given by intraperitoneal injection five times per week [13]. Tumor volume was monitored by measuring luciferase signals using an IVIS optical imaging system (In Vivo Imaging System; Xenogen, Alameda, CA). All animal procedures were conducted under regulations of the Division of Laboratory Animal Medicine at The University of Texas MD Anderson Cancer Center. Animal protocols (Protocol Number 190511133) were reviewed and approved by the Institutional Animal Care and Use Committee at The University of Texas MD Anderson Cancer Center.

EndoCD protein labeling

The Qdot605 Antibody Conjugation Kit (Q22-001MP, Invitrogen) was used to label purified EndoCD.

Intravital two-photon microscopy

Human pancreatic cancer cells AsPC1 or mouse stromal-enriched PDAC MP1070 cells were inoculated in mice pancreas. Once tumors reached approximately 5-10 mm in diameter,

mice were anesthetized, tail-vein catheterized, and pancreatic tumors were identified and exteriorized through a laparotomy. Body temperature was kept at 37°C throughout the experiments using a heating pad. The upper midline laparotomy was made as short as possible (< 15 mm). The pancreatic tumor was then transferred onto a soft-tissue immobilization system (VueBio Technology, Pearland, TX). The organ stabilizer minimized the micro-vibration of the observed area caused by heart beat and respiratory motion. Two-photo microscopy was performed using an upright multiphoton microscope 7MP (Carl Zeiss, LSM 7MP, NY) with a coherent pulsed Ti:Sapphire laser source (pulse width: 140 fs, repetition rate: 80 MHz; Coherent, Santa Clara, CA). An anesthetized mouse was placed on the microscope stage. The several lenses of the microscope provide the long working distances required for *in vivo* analysis. A mean laser power at the sample was between 10-40 mW, depending on the depth of imaging. Microscope objective lenses used in this study were 10X and 20X Plan Achromat lenses (numerical aperture of 0.45 and 0.8, respectively). Images were acquired with 1024 x 1024 pixels. Two-photon fluorescence signals were collected by an internal detector at an excitation wavelength at 910 nm to enable the simultaneous acquisition of the dextran-FITC signal and the Qdot605-EndoCD signal. The surface of the pancreatic tumor was initially screened at lower magnifications by setting out the *X/Y* plane and adjusting the *Z* axis manually to detect the optimal observation area containing blood vessels. The imaging depth or imaging stack was determined arbitrarily to allow real-time visualization of the relative distribution of Qdot605-labeled EndoCD *in vivo*. Data were analyzed using the Zen 2011 software package.

Trypsin-, chymotrypsin-, and elastase-like proteinase activities

Protease activity in serum of patients was measured as previously described [21]. Benzoylarginyl-p-nitroanilide hydrochloride (BAPNA, Sigma- Aldrich), N-succinyl-L-phenylalanine-p-nitroanilide (SPNA, Sigma- Aldrich), N-succinyl-alanine-alanine-proline-leucine-p-nitroanilide (SAAPLPNA, Sigma-Aldrich) substrates were used to measure trypsin-, chymotrypsin-, and elastase-like enzyme activity, respectively.

Serum samples from 10 patients with PDAC and 10 non-cancer healthy controls were drawn from a previously conducted case control study on PDAC at MD Anderson. An informed consent was obtained from each study participant, and the study was approved by the Institutional Review Board of MD Anderson.

Immunofluorescence staining

Frozen sections (4 mm) were fixed in cold 100% acetone for 5 min and then air-dried. After immersion in 1× PBS for 15 min, the slides were incubated with rat monoclonal anti-CD31 antibody, anti-CD45 antibody (BD Biosciences, San Jose, CA), or rabbit polyclonal alpha smooth muscle actin antibody (α-SMA; GeneTex, Irvine, CA) at room temperature for 1 hr, rinsed with 1× PBS, and then incubated with goat anti-rat immunoglobulin G conjugated to Texas Red (1:200; Jackson ImmunoResearch Laboratory, West Grove, PA) in the dark at ambient temperature for 60 min. For apoptosis assay, tissue sections were incubated with proteinase K (20 mg/ml in 10 mM Tris-HCl, pH 7.4-8.0, for 15 min at 37°C), permeabilized in 0.1% Triton-X-100 in 0.1% sodium citrate, and then labeled with the TUNEL (deoxynucleotide transferase-mediated dUTP-biotin nick end labeling) reaction mixture (Promega, Madison, WI) according to the manufacturer's protocol. Briefly, biotinylated nucleotide mix and TdT enzyme were added and incubated at 37°C for 1 hr. The slides were washed in PBS, blocked in hydrogen peroxide, incubated in streptavidin horseradish peroxidase, developed in 3,30-diaminobenzidine, and then counterstained with hematoxylin. In each sample, each signal was randomly counted in 5 fields counted under a microscope.

Small animal magnetic resonance imaging (MRI)

MRI was carried out as previously described [22]. Mice were anesthetized with isoflurane in a circulatory heating stage throughout the procedure. The dose was adjusted to maintain a respiratory rate between 20 and 50 breaths per minute. MRI of the pancreatic tumor was conducted with a Bruker 4.7T scanner located in the Small Animal Imaging Facility at the University of Texas MD Anderson Cancer Center.

Ultrasound imaging

All animals were imaged with a high-frequency small-animal ultrasound system (Vevo® 2100, FUJIFILM VisualSonics) utilizing a 21-MHz linear ultrasound array (LZ-250, FUJIFILM Visual-Sonics). During imaging studies, animals were kept anesthetized with 2.0% isoflurane with a 1.5 L/min medical air flow rate, and their body temperature was moderated with a heated imaging platform maintained at 36°C. The imaging focus (16 mm) and the time-gain-control settings were kept constant across all imaging acquisitions. Doppler and nonlinear contrast imaging studies were conducted twice on each mouse, once 10 days after tumor cell inoculation but before treatment initiation and once 18 days after cell inoculation and 8 days following treatment initiation. A matching B-mode ultrasound frame was acquired for each acquired Doppler or nonlinear contrast imaging frame. Tumor margins were manually segmented based on the B-mode data set for post-processing.

Nonlinear contrast imaging

The transducer array was translated to an imaging slice near the midsection of the tumor that contained the largest tumor cross-section. Nonlinear contrast imaging parameters were as follows for all acquisitions: gain = 15 dB; gate = 5; power = 6%; beamwidth = 'Standard'; frame rate = 8 fps. Fifty microliters of untargeted microbubble contrast (MicroMarkerTM, Bracco Group) were administered through a bolus tail-vein injection at an infusion rate of 40 µl/s. Imaging acquisition was initiated two seconds prior to the injection and continued for an additional 100 seconds. Output parameters, i.e., rise time (RT), time to peak (TTP) and wash-in rate (WiR), were calculated using the VevoCQ(TM) (Bracco Group) software package across the full tumor cross-section.

Doppler imaging

The linear array was translated (0.152-mm step size) up to 15 mm in the elevation dimension to obtain a full volume acquisition of the tumor. Doppler imaging parameters were as follows for all acquisitions: PRF = 2 kHz; gate = 2; persistence = 'Med'; gain = 35 dB. Percent vascularity was calculated with the Vevo® LAB (FUJIFLIM VisualSonics) software tool based on
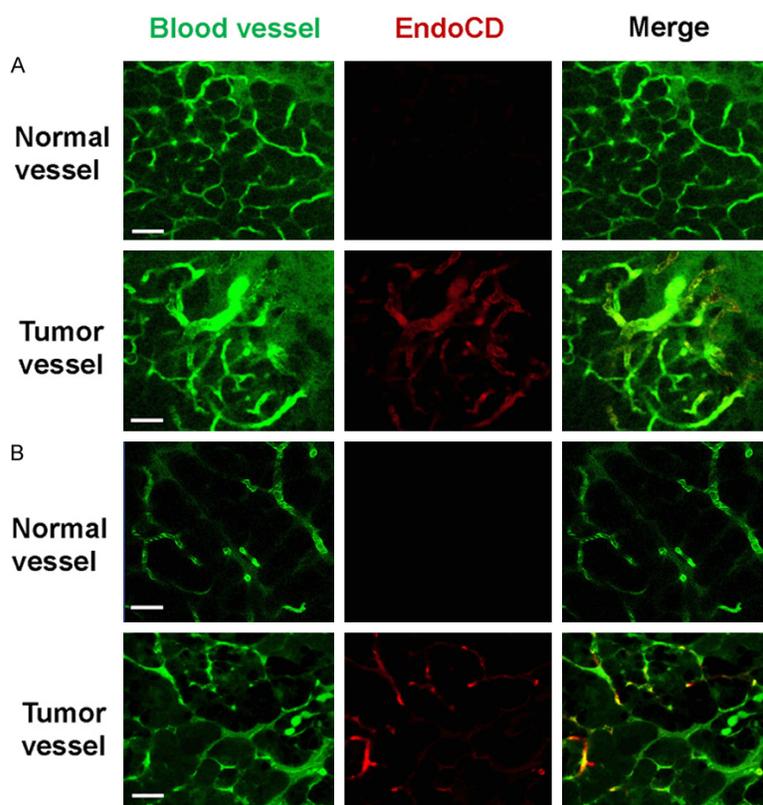
Figure 1. EndoCD targets pancreatic tumor vessels. Tumor-bearing mice were killed, and fluorescence-labeled EndoCD was injected via the tail vein. Mice were visualized by two-photon microscopy (LSM 7MP). The representative images shown were from the same mouse. A. AsPC1 model (human PDAC cells). B. MP1070 model (mouse stroma-enriched PDAC cells). Vessels were visualized by green staining (FITC-dextran), and EndoCD was visualized by red staining (Qdot605-EndoCD). Scale bar, 50 μm. The associated time-lapse videos are shown in Movies S1 and S2.

the total number of voxels-containing Doppler signal relative to the overall segmented tumor volume.

Masson's trichrome staining

Masson's trichrome staining solution was purchased from Sigma. Tissue section was rehydrated and incubated in Bouin's Solution at room temperature overnight. Samples were washed in running tap water for 5 min to remove the yellow color from the section, stained in Weigert's Iron Hematoxylin Solution for 5 min, washed again in running tap water for 5 min, and then stained in Biebrich Scarlet-Acid Fuchsin for 5 min. Slides were then placed in phosphomolybdic/phosphotungstic acid solution for 10 min, transferred to Aniline blue for 5 min, placed in 1% acetic acid solution for 3 min, and then rinsed in distilled water. Finally, the

section was washed with 1% acetic acid for 1 minute and rinsed in distilled water.

Statistical analysis

Statistical significance between groups was analyzed using a Student's t test or one-way or 2-way ANOVA. Survival was analyzed using a Kaplan-Meier plot, and log-rank test (Mantel-Cox test). A *P* value of less than 0.05 was considered statistically significant and is henceforth indicated by an asterisk.

Results

EndoCD preferentially targets pancreatic tumor vessels

Although endostatin is known to bind to integrin receptors that are expressed on tumor endothelial cells [23], it was not clear whether endostatin has tumor-targeting ability in the stroma-enriched PDAC. We therefore established orthotopic models of PDAC in mice by using the human AsPC1 or mouse MP1070 PDAC cells. MP1070 cells are known to generate prominent stroma, which is readily detectable by measuring the increase in collagen intensity [24] (Figure S1). FITC-labeled dextran was injected into tumor-bearing mice to mark the vessels by green fluorescence, and then Qdot605-labeled EndoCD was systemically delivered via tail vein catheterization [25] for the duration of imaging. The relative distribution of EndoCD in the vasculature of tumor and normal pancreatic tissues of each mouse was monitored by two-photon microscopy. As shown in **Figure 1**, Qdot605-labeled EndoCD bio-conjugates accumulated in the tumor vessels in larger quantities than in normal pancreatic vessels (Movies S1 and S2). These findings demonstrated EndoCD's selective targeting of tumor vessels (as opposed to normal vessels) in orthotopic models of PDAC using either human or mouse PDAC cells. The findings also

Figure 2. Resveratrol prolongs EndoCD protein stability and sensitizes cells to the killing effect of EndoCD by inhibiting chymotrypsin-like proteinase activity. A. Pancreatic cancer cell lines were treated with different doses of EndoCD/5-FC and with or without 10 μM resveratrol (Resv). Cell viability was determined by MTT assay. The viability of cells treated with 5-FC alone was set as 100%. Synergistic effects are indicated by combination index (CI) values. B. EndoCD was injected into mice, and resveratrol was orally administered every day. Protein concentration was

measured in sera by ELISA and normalized to the concentration measured on day 0. C. Mouse sera were incubated with EndoCD/5-FC, resveratrol, or EndoCD/5-FC/resveratrol for 5 days and then added to pancreatic cancer cells (see Materials and Methods). The viability of cells added 5-FC alone was set as 100%. D. Trypsin-, chymotrypsin-, and elastase-like activities in mouse sera treated with or without 10 µM resveratrol after 48 hr. E. Chymotrypsin A protein activity at different doses of resveratrol. F. Inducible Kras GEMM. Chymotrypsin-like proteinase activities in sera of mice with doxycycline-induced PDAC and control mice (without PDAC) from the same litter (n = 10). G. Chymotrypsin-like proteinase activities in sera from healthy individuals and PDAC patients (n = 10). OD, optical density.

suggest that EndoCD possesses tumor vessel-targeting potential even in a stroma-enriched PDAC microenvironment.

EndoCD/5-FC inhibits human pancreatic tumor growth in vitro and in vivo

To assess the therapeutic potential of EndoCD/5-FC, we first determined the cytotoxic effect of EndoCD/5-FC in culture-based studies using AsPC1/luc cells stably expressing luciferase. As shown in Figure S2A, EndoCD/5-FC decreased tumor cell viability in a dose-dependent manner. In addition, in the human orthotopic model of PDAC, 1 week after injection of AsPc1/luc cells, EndoCD (7.5 or 60 mg/kg) was administered by intravenous injection followed by intraperitoneal injection of 5-FC (500 mg/kg) later. EndoCD/5-FC inhibited tumor growth in a dose-dependent manner (Figure S2B, *P* < 0.05). These results indicate that EndoCD/5-FC inhibits pancreatic cancer cell viability and suppresses tumor growth.

The combination of EndoCD/5-FC and resveratrol induces a synergistic killing effect on PDAC cells

Several studies have reported that resveratrol sensitizes tumor cells to multiple chemotherapeutic agents, including 5-FU [17]. A high concentration of 5-FU was generated by EndoCD/5-FC to induce a bystander effect in the tumor microenvironment [15]. To determine the therapeutic effect of the EndoCD/5-FC/resveratrol combination, we first tested the cell-killing effect of resveratrol on pancreatic cancer cells (Figure S3). The results revealed that resveratrol inhibits pancreatic cancer cells in a dose-dependent manner and the minimal activity of resveratrol with an IC$_{10-20}$ of 10 µM was selected for combination. The combination of resveratrol (10 µM) and EndoCD/5-FC (at a dose of 2.5 µM, which is lower than the effective dose of 5 µM in Figure S2A) caused a significantly greater reduction in cell viability than EndoCD/5-FC alone in multiple cancer cell lines, with a combination index [19] lower than 1

(**Figure 2A**), indicating that EndoCD/5-FC combined with resveratrol has a synergistic killing effect on PDAC cells.

Resveratrol improves the pharmacokinetics of EndoCD ex vivo and in vivo

Previous studies indicated that a high concentration of resveratrol (200 µM) sensitizes colorectal cancer cells to 5-FU-mediated apoptosis via caspase-6 activation [26]. We observed similar results in PDAC cells (Figure S4). Notably, a low dose of resveratrol (10 µM), which induces synergistic chemosensitization to EndoCD/5-FC, was not associated with caspase-6 activation (Figure S4), suggesting the existence of an unknown mechanism of action of resveratrol at low doses. Because a major limitation of the clinical utility of endostatin and EndoCD is their short half-life in serum (6 hr and 2-3 days, respectively), we assessed whether resveratrol improves the pharmacokinetics of EndoCD in serum. Indeed, resveratrol prolonged the stability of EndoCD in circulation in mice. These studies were supported by *ex vivo* protein-serum mixing experiments in which purified His-tagged EndoCD, with or without resveratrol, was incubated with fresh mouse serum and monitored over several days. Western blot analysis using the anti-His-tag antibody showed that resveratrol increased the stability of the His-tagged EndoCD in the presence of mouse serum (Figure S5A). In addition, results from an ELISA indicated that resveratrol also delayed degradation of EndoCD in the blood circulation of mice (**Figure 2B**). We estimated that resveratrol extended the half-life of EndoCD to up to 1 week, which is comparable to the half-lives of clinically effective biologics such as therapeutic antibodies. The ability of resveratrol to prolong protein stability was also observed with other anti-cancer drugs, such as interferon gamma and trastuzumab (Figure S5B and S5C). Collectively, our data indicate that resveratrol appears to use an unknown mechanism to stabilize protein therapeutics in the presence of serum.
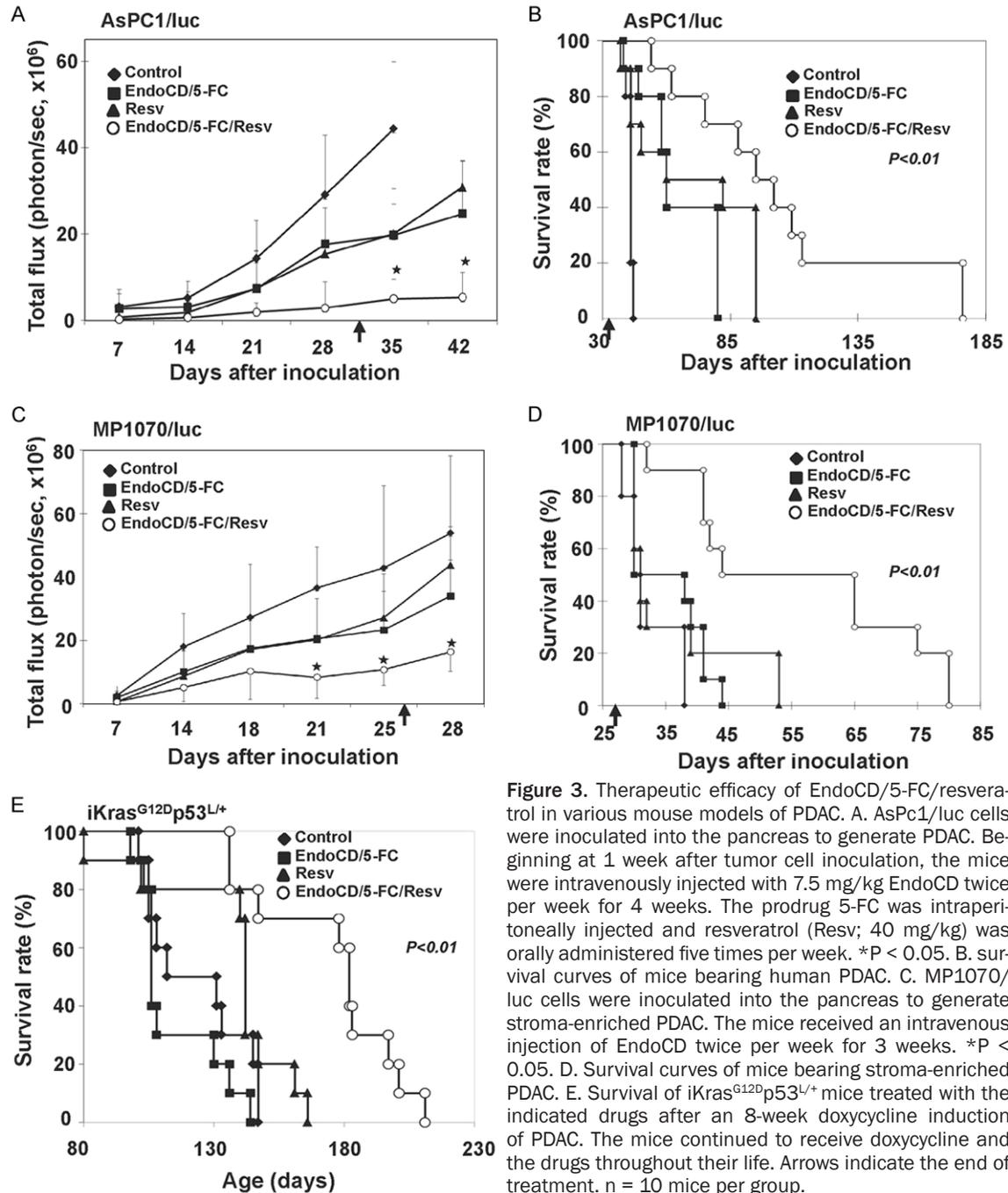
Figure 3. Therapeutic efficacy of EndoCD/5-FC/resveratrol in various mouse models of PDAC. A. AsPc1/luc cells were inoculated into the pancreas to generate PDAC. Beginning at 1 week after tumor cell inoculation, the mice were intravenously injected with 7.5 mg/kg EndoCD twice per week for 4 weeks. The prodrug 5-FC was intraperitoneally injected and resveratrol (Resv; 40 mg/kg) was orally administered five times per week. *P < 0.05. B. survival curves of mice bearing human PDAC. C. MP1070/luc cells were inoculated into the pancreas to generate stroma-enriched PDAC. The mice received an intravenous injection of EndoCD twice per week for 3 weeks. *P < 0.05. D. Survival curves of mice bearing stroma-enriched PDAC. E. Survival of iKras^{G12D}p53$^{L/+}$ mice treated with the indicated drugs after an 8-week doxycycline induction of PDAC. The mice continued to receive doxycycline and the drugs throughout their life. Arrows indicate the end of treatment. n = 10 mice per group.

Resveratrol reduces chymotrypsin-like proteinase activity

We next sought to determine whether the resveratrol-induced stability of EndoCD translates into improved therapeutic efficacy. We first determined the killing effect of the combination by an *ex vivo* serum co-culture assay in which pancreatic cancer cells were exposed to resveratrol, EndoCD, or a combination of EndoCD and resveratrol that had been pre-incubated in mouse serum for 7 days. By day 5, the amount of EndoCD decreased by 70%, whereas in the presence of resveratrol, EndoCD levels remained relatively unchanged ([Figure S5A]). Correspondingly, the EndoCD/5-FC/resveratrol combination that had been preincubated with mouse serum showed more potent cell killing activities than the similarly preincubated EndoCD/5-FC combination (**Figure 2C**). The finding of resveratrol-induced EndoCD stabilization and the associated increase in cytotoxic

effect prompted us to explore the mechanistic basis of resveratrol action. Serum contains various types of proteinases that break down proteins [27], and therefore, it is possible that resveratrol stabilizes EndoCD by inhibiting proteinase activities. To investigate this possibility, specific trypsin-, chymotrypsin-, or elastase-like peptides, with or without resveratrol, were co-cultured with mouse serum. We observed that resveratrol reduced chymotrypsin-like but not trypsin- or elastase-like proteinase activities (**Figure 2D**). The specific inhibitory effect of resveratrol against chymotrypsin-like proteinase was further demonstrated by a decrease in the activity of chymotrypsin A proteinase toward its substrate N-succinyl-L-phenylalanine-p-nitroanilide in the presence of resveratrol (**Figure 2E**).

We also examined serum chymotrypsin-like proteinase activity in a genetically engineered mouse model (GEMM) carrying a doxycycline-inducible $Kras^{G12D}$ mutation and a conditional p53 mutation (designated $iKras^{G12D}p53^{L/+}$), which recapitulates the hallmarks of PDAC, including a stroma-enriched tumor microenvironment, and develops tumors spontaneously 77-175 days after doxycycline induction [5]. We collected sera from mice with doxycycline-induced PDAC and control mice (without PDAC) from the same litter and subjected the sera to a chymotrypsin-like specific substrate. We found that chymotrypsin-like proteinase activity was higher in mice bearing PDAC than in control mice (**Figure 2F**). This finding was further validated in the sera of PDAC patients, which had higher chymotrypsin-like proteinase activity than sera from healthy individuals (**Figure 2G**). Collectively, these results suggest that resveratrol stabilizes EndoCD in serum by reducing chymotrypsin-like proteinase activity and has a synergistic therapeutic effect in combination with EndoCD/5-FC.

EndoCD/5-FC/resveratrol has potent anti-cancer efficacy in various PDAC models

Since it has been documented that stroma decreases the response to treatment in PDAC patients [7, 28], we evaluated the EndoCD/5-FC/resveratrol combination in a human xenograft model of AsPC1/luc PDAC containing a small amount of stroma and in a mouse model of stroma-enriched MP1070/luc PDAC. Mice bearing human AsPC1/luc tumors were treated with EndoCD (7.5 mg/kg) twice per week for 4

weeks by intravenous injection in combination with 5-FC (500 mg/kg) administered by intraperitoneal injection and/or resveratrol (40 mg/kg five times per week for 4 weeks) administered orally (**Figure 3A-D**). In agreement with the results from the *in vitro* and *ex vivo* cell-killing assays, the EndoCD/5-FC/resveratrol combination resulted in markedly greater tumor growth inhibition than either treatment alone or the vehicle control. Thus, on day 28, the rates of tumor growth inhibition by EndoCD/5-FC, resveratrol, and EndoCD/5-FC/resveratrol were 40, 48, and 90%, respectively (**Figure 3A**). In addition, EndoCD/5-FC/resveratrol resulted in a median survival of 90 days compared to 41 days for the vehicle control (**Figure 3B**). Interestingly, the stroma-enriched environment in the MP1070/luc tumors did not affect the therapeutic potential of the EndoCD/5-FC/resveratrol combination. In mice with MP1070/luc tumors, EndoCD/5-FC/resveratrol reduced tumor growth by ~70% by day 28 in comparison with the control group and resulted in median survival of 44 days compared with 30 days for the controls (46.7% increase) (**Figure 3C** and **3D**). EndoCD/5-FC alone and resveratrol alone inhibited tumor growth by only 27% and 19%, respectively.

We further validated the efficacy of the EndoCD/5-FC/resveratrol regimen in the $iKras^{G12D}p53^{L/+}$ GEMM. Mice were administered EndoCD/5-FC, resveratrol, or EndoCD/5-FC/resveratrol after an 8-week doxycycline induction. The median survival durations were 106, 105, 142, and 182 days for vehicle control-, EndoCD/5-FC-, resveratrol-, and EndoCD/5-FC/resveratrol-treated mice, respectively. Thus, EndoCD/5-FC/resveratrol resulted in median survival that was 72% longer than median survival in the vehicle control group (**Figure 3E**). The results indicate that the EndoCD/5-FC/resveratrol combination substantially improves survival in mice with PDAC. It is worthwhile to mention that all three mouse models of PDAC harbor *Kras*-mutated tumors. Thus, our findings demonstrate that the EndoCD/5-FC/resveratrol combination has potent anti-cancer efficacy in PDAC orthotopic models and GEMMs.

EndoCD/5-FC/resveratrol destroys the stroma in the tumor microenvironment

The efficacy of the EndoCD/5-FC/resveratrol combination in stroma-enriched PDAC models
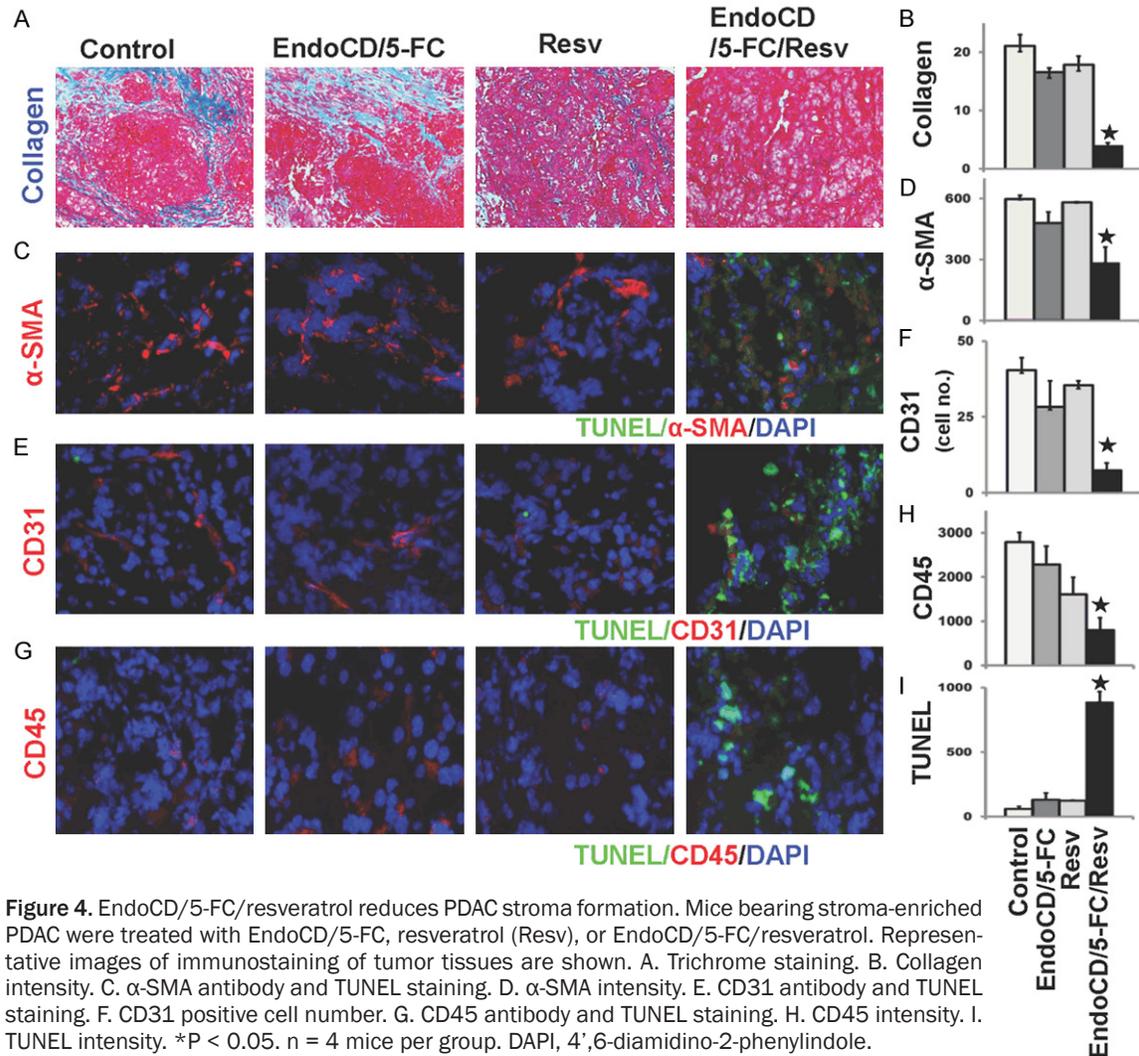
Figure 4. EndoCD/5-FC/resveratrol reduces PDAC stroma formation. Mice bearing stroma-enriched PDAC were treated with EndoCD/5-FC, resveratrol (Resv), or EndoCD/5-FC/resveratrol. Representative images of immunostaining of tumor tissues are shown. A. Trichrome staining. B. Collagen intensity. C. α-SMA antibody and TUNEL staining. D. α-SMA intensity. E. CD31 antibody and TUNEL staining. F. CD31 positive cell number. G. CD45 antibody and TUNEL staining. H. CD45 intensity. I. TUNEL intensity. *P < 0.05. n = 4 mice per group. DAPI, 4',6-diamidino-2-phenylindole.

prompted us to investigate the effect of this combination on stroma, which consists of several cell types, including pancreatic stellate cells (PSCs), endothelial cells, and immune cells, and the extracellular matrix [29]. Tumor samples were harvested and subjected to five different analyses: TUNEL assay (to measure apoptosis), α-SMA staining (to detect an activated PSCs marker), CD31 staining (to identify endothelial cells), CD45 staining (to detect leukocytes), and trichrome staining (to measure the amount of collagen in PDAC). Our results indicated that the EndoCD/5-FC/resveratrol combination reduced all of the following: the amount of collagen (**Figure 4A** and **4B**), the number of activated PSCs (decreased α-SMA intensity; **Figure 4C** and **4D**), the density of tumor vessels (loss of CD31 signal intensity; **Figure 4E** and **4F**), and the number of leuko-

cytes (decreased CD45 intensity; **Figure 4G** and **4H**). Moreover, EndoCD/5-FC/resveratrol also induced apoptosis of stroma cells, including PSCs, endothelial cells, and immune cells, in addition to tumor cells (**Figure 4I**). These results indicate that EndoCD/5-FC/resveratrol combination therapy destroys the cells that make up the stroma in the tumor microenvironment via a chemotherapeutic bystander effect.

The chemotherapeutic bystander effect decreases tumor vasculature and subsequently reduces blood perfusion in PDAC

Angiogenesis is known to serve an important role in fostering PDAC tumor growth [7]. To determine whether the chemotherapeutic bystander effect induced by EndoCD/5-FC/resveratrol affects tumor blood flow associated with
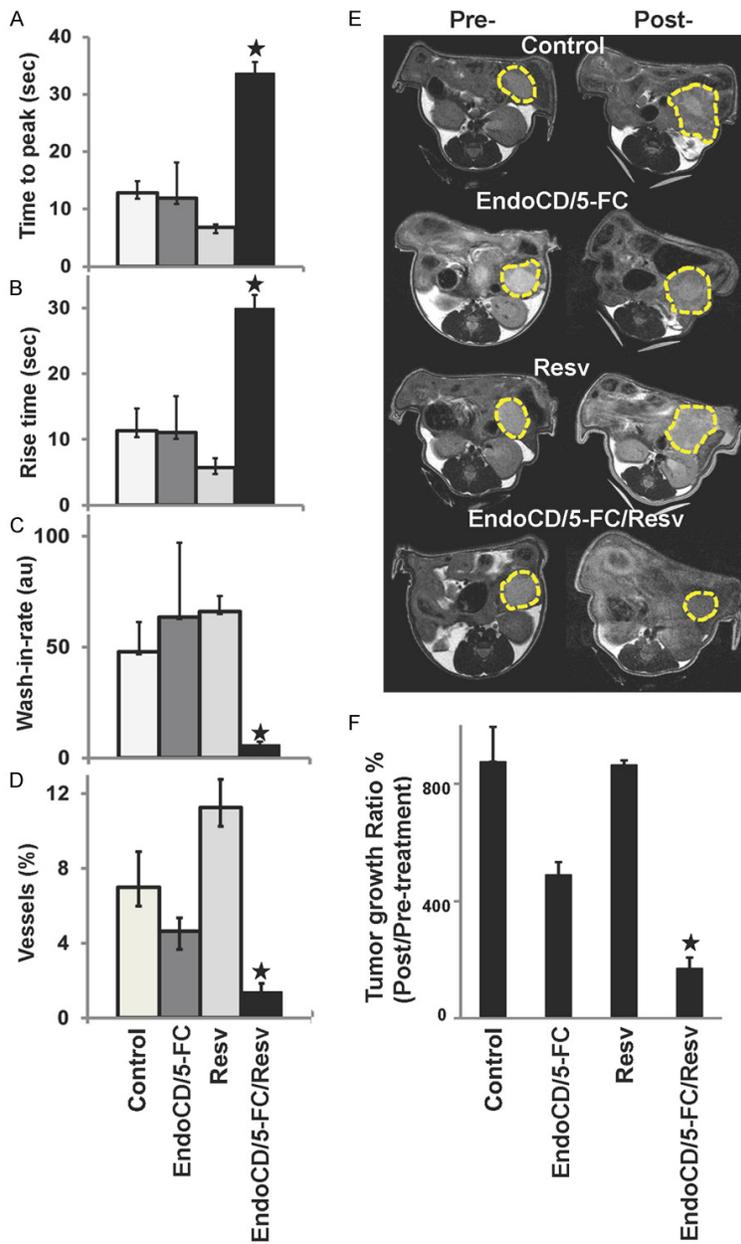
Figure 5. EndoCD/5-FC/resveratrol reduces the kinetics of tumor blood flow. Blood flow parameters (A-C) and percentages of tumor vessel density (D) were calculated by high-frequency ultrasound. au, absorbance units; Resv, resveratrol. Tumors were located and measured by MRI, (E) representative pre- and post-treatment MRI images. Tumors are outlined in yellow. (F) tumor volume. *P < 0.05. n = 4 mice per group.

injected a bolus of a microbubble contrast agent into the mice via tail vein catheterization and assessed the dynamics of the agent with ultrasound-based harmonic imaging. Parameters representing the kinetics of blood flow in the tumor were calculated from time-intensity curves [31] (Movies S3, S4, S5, S6; see Materials and Methods). The parameters rise time (RT) and time to peak (TTP) parameters, which are both inversely related to tumor perfusion, were significantly higher in mice administered the combined treatment than in mice administered either EndoCD/5-FC or resveratrol alone or in mice administered the vehicle control, indicating that the contrast agent took longer to reach the tumor and attain maximum intensity. In addition, the wash-in rate, (WiR) calculated from the slope of the time-intensity curves, which indicates relative blood flow within the tumor, was the lowest in EndoCD/5-FC/resveratrol-treated mice. Together, these data show that Endo-CD/5-FC/resveratrol reduces the rate of blood flow into the tumor in mice more than either EndoCD/5-FC or resveratrol alone or the vehicle control (**Figure 5A-C** and Figure S6).

Angiogenesis is highly associated with increased blood flow and permeability, which enhances the accumulation of a contrast agent at the tumor site [32]. Therefore, we also investigated whether the EndoCD/5-FC/resveratrol combination reduces the blood flow rate by assessing the three-dimensional vessel density in the tumor with ultrasound-based color Doppler imaging. We found that vessel density was lower in tumors in mice treated with the EndoCD/5-FC/resveratrol combination than in mice treated with either EndoCD/5-FC or resveratrol alone or the vehicle control

angiogenesis, we treated mice bearing stroma-enriched PDAC with EndoCD/5-FC, resveratrol, or EndoCD/5-FC/resveratrol. Prior to administration of the drugs, mice were imaged with a high-frequency ultrasound system [30] to ensure that no parameters (see Materials and Methods) were significantly different. After 8 days of treatment, the mice were re-imaged. To measure the kinetics of tumor blood flow, we

(**Figure 5D** and <u>Figure S7</u>). This finding indicates that EndoCD/5-FC/resveratrol induces a chemotherapeutic bystander effect and thereby decreases tumor vasculature and subsequently reduces blood perfusion in PDAC. The marked decrease in PDAC tumor growth after the 8-day treatment was further validated by MRI (**Figure 5E** and **5F**). Collectively, these data suggest that resveratrol enhances the protein stability of the tumor-targeting EndoCD/5-FC and sensitizes PDAC tumors to the chemotherapeutic bystander effect of EndoCD/5-FC. The bystander effect leads to a breach in the stroma by inducing apoptosis of stromal composite cells, including endothelial cells, PSCs, leukocytes, and tumor cells, and results in tumor shrinkage (**Figure 6**).

Discussion

FOLFIRINOX (bolus and infusional 5-FU, leucovorin, irinotecan, and oxaliplatin) combination chemotherapy is currently approved by the Food and Drug Administration for treating advanced pancreatic cancer. However, the adverse effects caused by non-specific tumor targeting remain a concern in the clinic [33, 34]. In the current study, we have shown that EndoCD/5-FC selectively binds to pancreatic tumor vessels but not normal vessels, resulting in tumor-specific conversion of 5-FC to 5-FU, which effectively inhibits pancreatic cancer growth. Furthermore, the therapeutic efficacy of EndoCD/5-FC was enhanced by the addition of resveratrol, which increased the protein stability of EndoCD by reducing chymotrypsin-like proteinase activity and sensitized cancer cells to the killing effect of EndoCD/5-FC. The previously unidentified function of resveratrol in prolonging protein stability was also observed with the anti-cancer agents interferon gamma and trastuzumab. The higher level of proteinase activity in the sera of PDAC patients and mice with PDAC may render PDAC less sensitive to protein therapy, which raises an interesting possibility that this mechanism may have contributed to the failure of some clinical trials that utilized protein therapy. Our results indicate that the addition of resveratrol has the potential to address reduced protein half-life in serum. In addition to inducing apoptosis in endothelial cells, EndoCD/5-FC/resveratrol induced apoptosis in other cell types, including cancer cells, activated PSCs, and leukocytes.

The induction of apoptosis led to the inhibition of collagen formation and reduction of vessel density, demonstrating both the anti-tumor and the anti-fibrotic effects of this treatment.

Tumor angiogenesis plays a critical role in tumor growth and metastasis. The combination of bevacizumab (an anti-angiogenic agent) and gemcitabine (a chemotherapeutic drug) failed to lengthen survival in PDAC patients [35]. This lack of efficacy may be due to the cytostatic nature of the anti-angiogenic effect, in which cancer cells that are not killed by these drugs later develop an even more malignant phenotype, resulting in tumor invasion and metastasis [36]. In addition, the difference in the rate at which gemcitabine and bevacizumab inhibit tumor growth may produce an antagonistic effect due to the decrease in chemo-drug delivery caused by inhibition of angiogenesis. Although many approaches have been used to reduce drug resistance and increase therapeutic efficacy by combining anti-angiogenic drugs with chemotherapy, the cumulative toxicity of blocking angiogenesis limits the feasibility of such strategies [37]. The tumor-targeting EndoCD/5-FC fusion protein exerts a chemotherapeutic effect through tumor site-specific conversion of 5-FC to 5-FU. The elevated levels of 5-FU in the tumor mass [15] induced a bystander effect that killed endothelial, cancer, and stromal composite cells before the anti-angiogenesis effect could occur (**Figure 6**). In the presence of resveratrol, EndoCD remains longer in tumor endothelial cells and continues to convert 5-FU. Meanwhile, resveratrol sensitizes cells to 5-FU [17] by inducing a bystander effect in the tumor microenvironment before tumor vessels are destroyed. Therefore, this strategy may be able to overcome the low tumor-specific chemotherapeutic effect and the lack of stroma depletion activity that are associated with the gemcitabine/bevacizumab combination in PDAC treatment. Given that no effective therapy targeting *Kras* mutations is currently available, our finding that the EndoCD/5-FC/resveratrol combination inhibited tumor growth in mice harboring *Kras* mutations (AsPC1 and MP1070 cells and the *iKras*^{G12D}*p53*$^{L/+}$ GEMM) indicates that this combination has potential for treatment of PDAC and warrants investigation in a clinical setting.

There is growing evidence implicating stroma as a prognostic marker, with the activated stro-
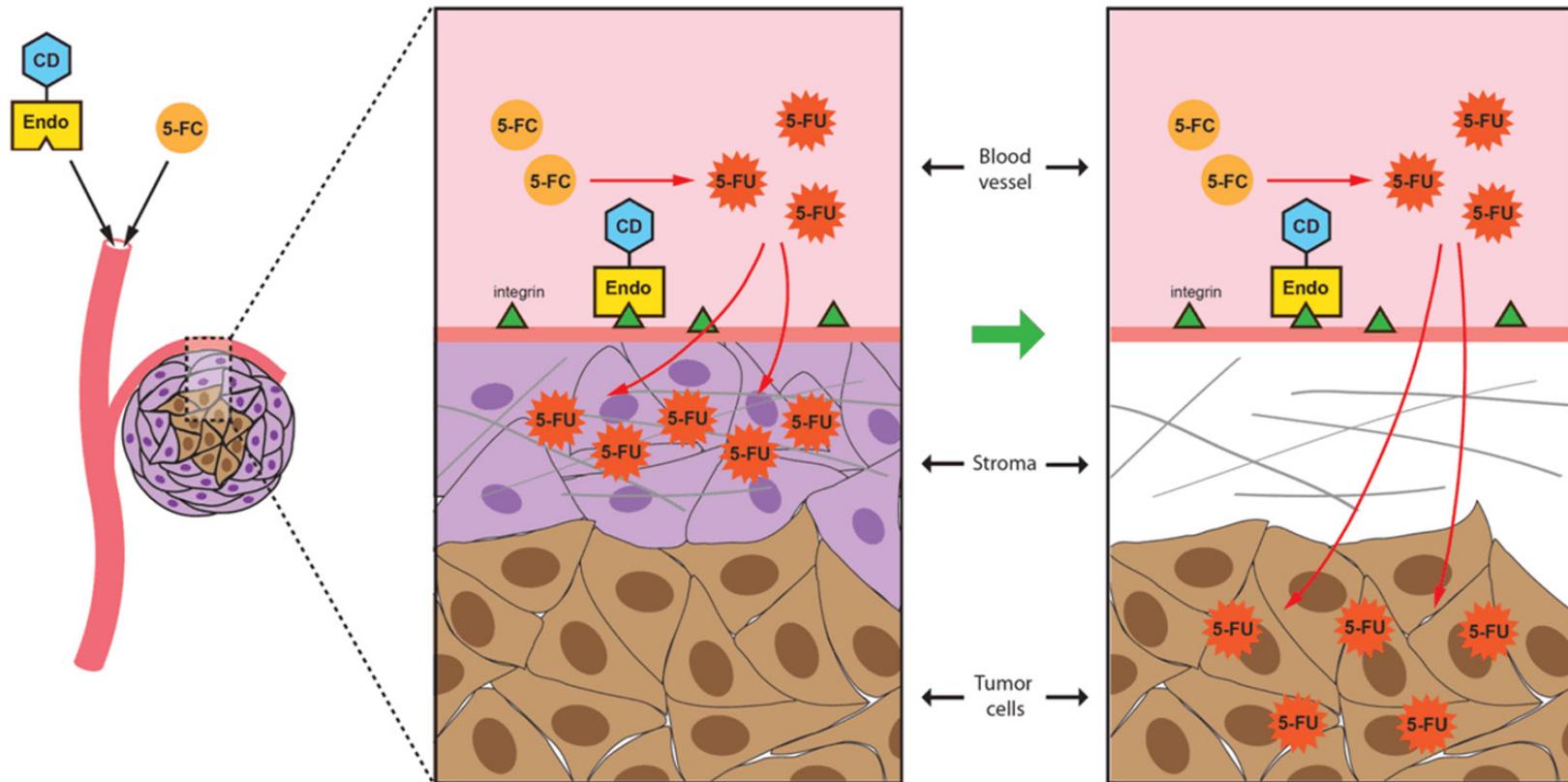
Figure 6. Proposed model of tumor-targeting EndoCD/5-FC exerting a chemotherapeutic bystander effect and penetrating the stroma to inhibit PDAC.

ma index (the ratio of the α-SMA-stained area to the collagen-stained area) potentially predicting PDAC patient survival [7]. Patients with dominantly inert (low α-SMA and collagen) or dormant (low α-SMA and high collagen) PDAC stroma had significantly better survival [38]. Our data indicate that EndoCD/5-FC/resveratrol-treated mice had lower α-SMA and collagen than control mice and that these decreases correlated with lower tumor volume as measured by different *in vivo* live imaging methods. These findings suggest that the EndoCD/5-FC/resveratrol combination is an effective treatment strategy that has potential to benefit PDAC patient survival.

In addition to being used to monitor tumor volume, current advances in noninvasive imaging techniques can be used to determine a drug's targeting effect. Contrast-enhanced ultrasound increases imaging sensitivity and content and is an important clinical tool for lesion detection and cancer diagnosis [39]. Our ultrasound results indicate that the EndoCD/5-FC/resveratrol combination affected specifically the parameters rise time, time to peak, and wash-in rate. While these parameters are time dependent, they tend to be less dependent on the received echo power and contrast agent concentration, which are can be difficult to control for in a clinical setting. Therefore, we conclude that these ultrasound-based imaging techniques (albeit at lower, clinical transmit frequencies) warrant translation into imaging-guided clinical trials of the EndoCD/5-FC/resveratrol combination therapy to predict the efficacy of this therapy against PDAC.

Disclosure of conflict of interest

M.-C. Hung is an inventor on a patent for the EndoCD fusion protein. M.-C. Hung and C.-T. Chen are inventors on a patent for the prolonged protein stabilization by resveratrol.

Address correspondence to: Mien-Chie Hung, Department of Molecular and Cellular Oncology, The University of Texas MD Anderson Cancer Center, 1515 Holcombe Boulevard, Unit 108, Houston, TX 77030, USA. E-mail: mhung@mdanderson.org

References

[1] Raimondi S, Maisonneuve P and Lowenfels AB. Epidemiology of pancreatic cancer: an overview. Nat Rev Gastroenterol Hepatol 2009; 6: 699-708.

[2] Erkan M, Hausmann S, Michalski CW, Fingerle AA, Dobritz M, Kleeff J and Friess H. The role of stroma in pancreatic cancer: diagnostic and therapeutic implications. Nat Rev Gastroenterol Hepatol 2012; 9: 454-467.

[3] Sirivatanauksorn V, Sirivatanauksorn Y and Lemoine NR. Molecular pattern of ductal pancreatic cancer. Langenbecks Arch Surg 1998; 383: 105-115.

[4] Karamitopoulou E. Tumor budding cells, cancer stem cells and epithelial-mesenchymal transition-type cells in pancreatic cancer. Front Oncol 2012; 2: 209.

[5] Ying H, Kimmelman AC, Lyssiotis CA, Hua S, Chu GC, Fletcher-Sananikone E, Locasale JW, Son J, Zhang H, Coloff JL, Yan H, Wang W, Chen S, Viale A, Zheng H, Paik JH, Lim C, Guimaraes AR, Martin ES, Chang J, Hezel AF, Perry SR, Hu J, Gan B, Xiao Y, Asara JM, Weissleder R, Wang YA, Chin L, Cantley LC and DePinho RA. Oncogenic Kras maintains pancreatic tumors through regulation of anabolic glucose metabolism. Cell 2012; 149: 656-670.

[6] Wang Y, Kaiser CE, Frett B and Li HY. Targeting mutant KRAS for anticancer therapeutics: a review of novel small molecule modulators. J Med Chem 2013; 56: 5219-5230.

[7] Waghray M, Yalamanchili M, di Magliano MP and Simeone DM. Deciphering the role of stroma in pancreatic cancer. Curr Opin Gastroenterol 2013; 29: 537-543.

[8] Olive KP, Jacobetz MA, Davidson CJ, Gopinathan A, McIntyre D, Honess D, Madhu B, Goldgraben MA, Caldwell ME, Allard D, Frese KK, Denicola G, Feig C, Combs C, Winter SP,

Ireland-Zecchini H, Reichelt S, Howat WJ, Chang A, Dhara M, Wang L, Ruckert F, Grutzmann R, Pilarsky C, Izeradjene K, Hingorani SR, Huang P, Davies SE, Plunkett W, Egorin M, Hruban RH, Whitebread N, McGovern K, Adams J, Iacobuzio-Donahue C, Griffiths J and Tuveson DA. Inhibition of Hedgehog signaling enhances delivery of chemotherapy in a mouse model of pancreatic cancer. Science 2009; 324: 1457-1461.

[9] Ozdemir BC, Pentcheva-Hoang T, Carstens JL, Zheng X, Wu CC, Simpson TR, Laklai H, Sugimoto H, Kahlert C, Novitskiy SV, De Jesus-Acosta A, Sharma P, Heidari P, Mahmood U, Chin L, Moses HL, Weaver VM, Maitra A, Allison JP, LeBleu VS and Kalluri R. Depletion of Carcinoma-Associated Fibroblasts and Fibrosis Induces Immunosuppression and Accelerates Pancreas Cancer with Reduced Survival. Cancer Cell 2014; 25: 719-34.

[10] Rhim AD, Oberstein PE, Thomas DH, Mirek ET, Palermo CF, Sastra SA, Dekleva EN, Saunders T, Becerra CP, Tattersall IW, Westphalen CB, Kitajewski J, Fernandez-Barrena MG, Fernandez-Zapico ME, Iacobuzio-Donahue C, Olive KP and Stanger BZ. Stromal Elements Act to Restrain, Rather Than Support, Pancreatic Ductal Adenocarcinoma. Cancer Cell 2014; 25: 735-47.

[11] Kerbel R and Folkman J. Clinical translation of angiogenesis inhibitors. Nat Rev Cancer 2002; 2: 727-739.

[12] Xu F, Ma Q and Sha H. Optimizing drug delivery for enhancing therapeutic efficacy of recombinant human endostatin in cancer treatment. Crit Rev Ther Drug Carrier Syst 2007; 24: 445-492.

[13] Chung-Faye GA, Chen MJ, Green NK, Burton A, Anderson D, Mautner V, Searle PF and Kerr DJ. In vivo gene therapy for colon cancer using adenovirus-mediated, transfer of the fusion gene cytosine deaminase and uracil phosphoribosyltransferase. Gene Ther 2001; 8: 1547-1554.

[14] Ramnaraine M, Pan W, Goblirsch M, Lynch C, Lewis V, Orchard P, Mantyh P and Clohisy DR. Direct and bystander killing of sarcomas by novel cytosine deaminase fusion gene. Cancer Res 2003; 63: 6847-6854.

[15] Chen CT, Yamaguchi H, Lee HJ, Du Y, Lee HH, Xia W, Yu WH, Hsu JL, Yen CJ, Sun HL, Wang Y, Yeh ET, Hortobagyi GN and Hung MC. Dual targeting of tumor angiogenesis and chemotherapy by endostatin-cytosine deaminase-uracil phosphoribosyltransferase. Mol Cancer Ther 2011; 10: 1327-1336.

[16] Shankar S, Singh G and Srivastava RK. Chemoprevention by resveratrol: molecular mechanisms and therapeutic potential. Front Biosci 2007; 12: 4839-4854.

[17] Gupta SC, Kannappan R, Reuter S, Kim JH and Aggarwal BB. Chemosensitization of tumors by resveratrol. Ann N Y Acad Sci 2011; 1215: 150-160.

[18] Chen CT, Chen YC, Yamaguchi H and Hung MC. Carglumic acid promotes apoptosis and suppresses cancer cell proliferation in vitro and in vivo. Am J Cancer Res 2015; 5: 3560-3569.

[19] Chou TC and Talalay P. Quantitative analysis of dose-effect relationships: the combined effects of multiple drugs or enzyme inhibitors. Adv Enzyme Regul 1984; 22: 27-55.

[20] Shankar S, Nall D, Tang SN, Meeker D, Passarini J, Sharma J and Srivastava RK. Resveratrol inhibits pancreatic cancer stem cell characteristics in human and KrasG12D transgenic mice by inhibiting pluripotency maintaining factors and epithelial-mesenchymal transition. PLoS One 2011; 6: e16530.

[21] Altshuler AE, Penn AH, Yang JA, Kim GR and Schmid-Schonbein GW. Protease activity increases in plasma, peritoneal fluid, and vital organs after hemorrhagic shock in rats. PLoS One 2012; 7: e32672.

[22] van Zijl PC, Jones CK, Ren J, Malloy CR and Sherry AD. MRI detection of glycogen in vivo by using chemical exchange saturation transfer imaging (glycoCEST). Proc Natl Acad Sci U S A 2007; 104: 4359-4364.

[23] Folkman J. Antiangiogenesis in cancer therapy--endostatin and its mechanisms of action. Exp Cell Res 2006; 312: 594-607.

[24] Apte MV, Park S, Phillips PA, Santucci N, Goldstein D, Kumar RK, Ramm GA, Buchler M, Friess H, McCarroll JA, Keogh G, Merrett N, Pirola R and Wilson JS. Desmoplastic reaction in pancreatic cancer: role of pancreatic stellate cells. Pancreas 2004; 29: 179-187.

[25] Hedrich H and Bullock E. The Laboratory Mouse. in Elsevier Limited, Vol. Amsterdam 2004.

[26] Chan JY, Phoo MS, Clement MV, Pervaiz S and Lee SC. Resveratrol displays converse dose-related effects on 5-fluorouracil-evoked colon cancer cell apoptosis: the roles of caspase-6 and p53. Cancer Biol Ther 2008; 7: 1305-1312.

[27] Ayache S, Panelli M, Marincola FM and Stroncek DF. Effects of storage time and exogenous protease inhibitors on plasma protein levels. Am J Clin Pathol 2006; 126: 174-184.

[28] Lunardi S, Muschel RJ and Brunner TB. The stromal compartments in pancreatic cancer: Are there any therapeutic targets? Cancer Lett 2014; 343: 147-55.

[29] Chu GC, Kimmelman AC, Hezel AF and DePinho RA. Stromal biology of pancreatic cancer. J Cell Biochem 2007; 101: 887-907.

[30] Fuchs CS, Tomasek J, Yong CJ, Dumitru F, Passalacqua R, Goswami C, Safran H, dos

Santos LV, Aprile G, Ferry DR, Melichar B, Tehfe M, Topuzov E, Zalcberg JR, Chau I, Campbell W, Sivanandan C, Pikiel J, Koshiji M, Hsu Y, Liepa AM, Gao L, Schwartz JD, Tabernero J; REGARD Trial Investigators. Ramucirumab monotherapy for previously treated advanced gastric or gastro-oesophageal junction adenocarcinoma (REGARD): an international, randomised, multicentre, placebo-controlled, phase 3 trial. Lancet 2014; 383: 31-9.

[31] Sboros V, Averkiou M, Lampaskis M, Thomas DH, Silva N, Strouthos C, Docherty J and McNeilly AS. Imaging of the ovine corpus luteum microcirculation with contrast ultrasound. Ultrasound Med Biol 2011; 37: 59-68.

[32] Miles KA. Tumour angiogenesis and its relation to contrast enhancement on computed tomography: a review. Eur J Radiol 1999; 30: 198-205.

[33] Conroy T, Gavoille C, Samalin E, Ychou M and Ducreux M. The role of the FOLFIRINOX regimen for advanced pancreatic cancer. Curr Oncol Rep 2013; 15: 182-189.

[34] Conroy T, Desseigne F, Ychou M, Bouché O, Guimbaud R, Bécouarn Y, Adenis A, Raoul JL, Gourgou-Bourgade S, de la Fouchardière C, Bennouna J, Bachet JB, Khemissa-Akouz F, Péré-Vergé D, Delbaldo C, Assenat E, Chauffert B, Michel P, Montoto-Grillot C, Ducreux M; Groupe Tumeurs Digestives of Unicancer; PRODIGE Intergroup. FOLFIRINOX versus gemcitabine for metastatic pancreatic cancer. N Engl J Med 2011; 364: 1817-1825.

[35] Kindler HL, Niedzwiecki D, Hollis D, Sutherland S, Schrag D, Hurwitz H, Innocenti F, Mulcahy MF, O'Reilly E, Wozniak TF, Picus J, Bhargava P, Mayer RJ, Schilsky RL and Goldberg RM. Gemcitabine plus bevacizumab compared with gemcitabine plus placebo in patients with advanced pancreatic cancer: phase III trial of the Cancer and Leukemia Group B (CALGB 80303). J Clin Oncol 2010; 28: 3617-3622.

[36] Loges S, Mazzone M, Hohensinner P and Carmeliet P. Silencing or fueling metastasis with VEGF inhibitors: antiangiogenesis revisited. Cancer Cell 2009; 15: 167-170.

[37] Chen CT and Hung MC. Beyond anti-VEGF: dual-targeting antiangiogenic and antiproliferative therapy. Am J Transl Res 2013; 5: 393-403.

[38] Erkan M, Michalski CW, Rieder S, Reiser-Erkan C, Abiatari I, Kolb A, Giese NA, Esposito I, Friess H and Kleeff J. The activated stroma index is a novel and independent prognostic marker in pancreatic ductal adenocarcinoma. Clin Gastroenterol Hepatol 2008; 6: 1155-1161.

[39] Olson P, Chu GC, Perry SR, Nolan-Stevaux O and Hanahan D. Imaging guided trials of the angiogenesis inhibitor sunitinib in mouse models predict efficacy in pancreatic neuroendocrine but not ductal carcinoma. Proc Natl Acad Sci U S A 2011; 108: E1275-1284.
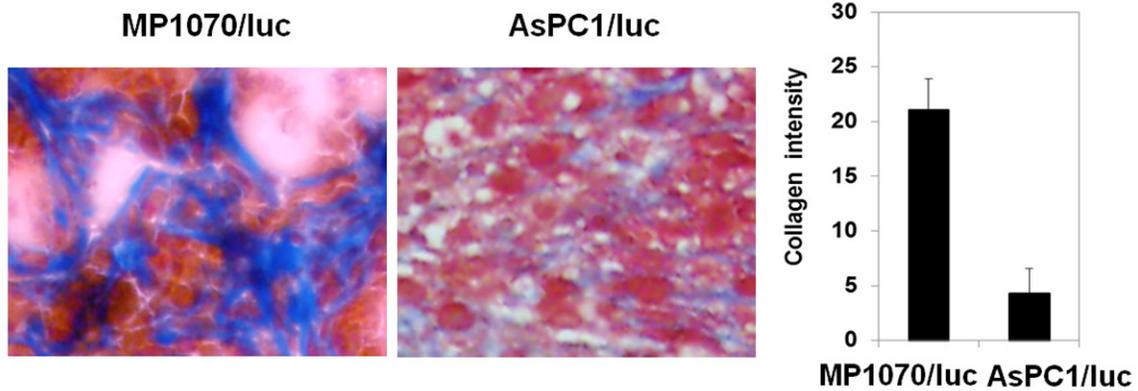
Figure S1. Collagen levels in human AsPC1 and mouse stromal-enriched MP1070 pancreatic cancer. MP1070/luc and AsPC1/luc PDAC cells were injected into the pancreas of mice, and tumor tissues were subjected to trichrome staining. Three mice per groups were orthotopically inoculated same amount of MP1070/luc and AsPC1/luc PDAC cells in pancreas, tumors were harvested in the same day to determine collagen level.
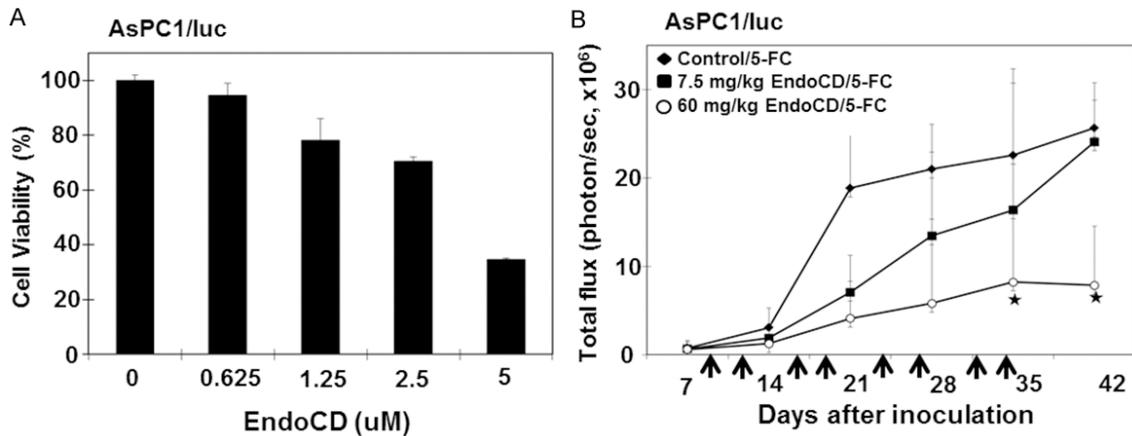
Figure S2. Therapeutic efficacy of EndoCD/5-FC in an orthotopic mouse model of human PDAC. A. Cell killing effect was assessed in AsPC1/luc cells treated with 200 µg/ml of 5-FC and various concentrations of EndoCD. The cell viability of 5-FC alone group was set as 100%. B. EndoCD proteins (7.5 mg/kg and 60 mg/kg) were injected intravenously twice per week. An hour after protein treatment, mice were given 500 mg/kg of 5-FC by intraperitoneal injection. Arrows represent protein treatment. ◆, Control/5-FC; ■, 7.5 mg/kg EndoCD/5-FC; ○, 60 mg/kg EndoCD/5-FC.
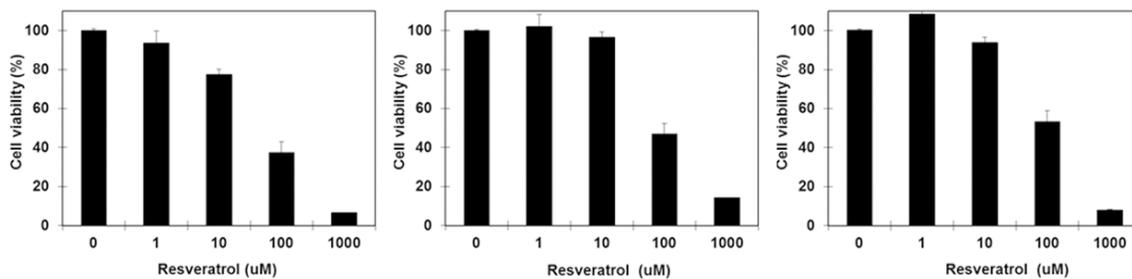
Figure S3. Cell killing effect of resveratrol. PanO2/luc, Capan1, and AsPC1/luc cells (From left to right) were treated with various concentrations of resveratrol. Resveratrol at the concentration of 10 µM was selected for combination treatment with EndoCD/5-FC.

1

AsPC1/luc

5-FU (IC$_{50}$)	−	−	−	−	+	+	+	+
Resveratrol (uM)	0	10	50	200	0	10	50	200

Pro-Caspase-6

Tubulin

| 1 | 2 | 3 | 4 | 5 | 6 | 7 | 8 |
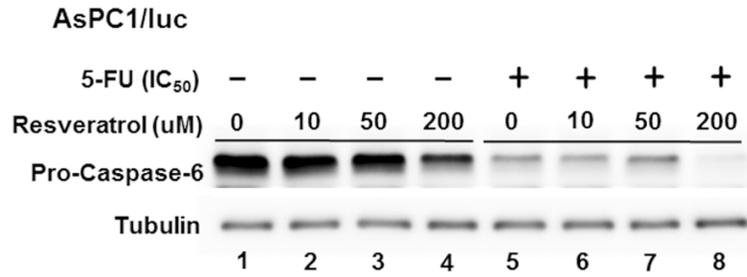
Figure S4. Levels of procaspase-6 after resveratrol/5-FU treatment. AsPC1 cells (1 × 10^6) were treated with resveratrol (0, 10, 50, 200 µM) or in combination with 5-FU (IC$_{50}$) for 72 hr. Cell lysates were subjected to Western blot analysis with anti-caspase-6 antibody. A decrease in procaspase-6 signal indicates that cells underwent apoptosis, as seen in the 5-FU treated cells (procaspase-6 signal decreased; lane 5 vs. lane 1). Resveratrol sensitized cells to 5-FU-mediated apoptosis in pancreatic cancer cells at a concentration of 200 µM (procaspase-6 signal decreased; lane 8 vs. lane 5) but not at 10 µM (procaspase-6 signal did not change significantly; lane 6 vs. lane 5).
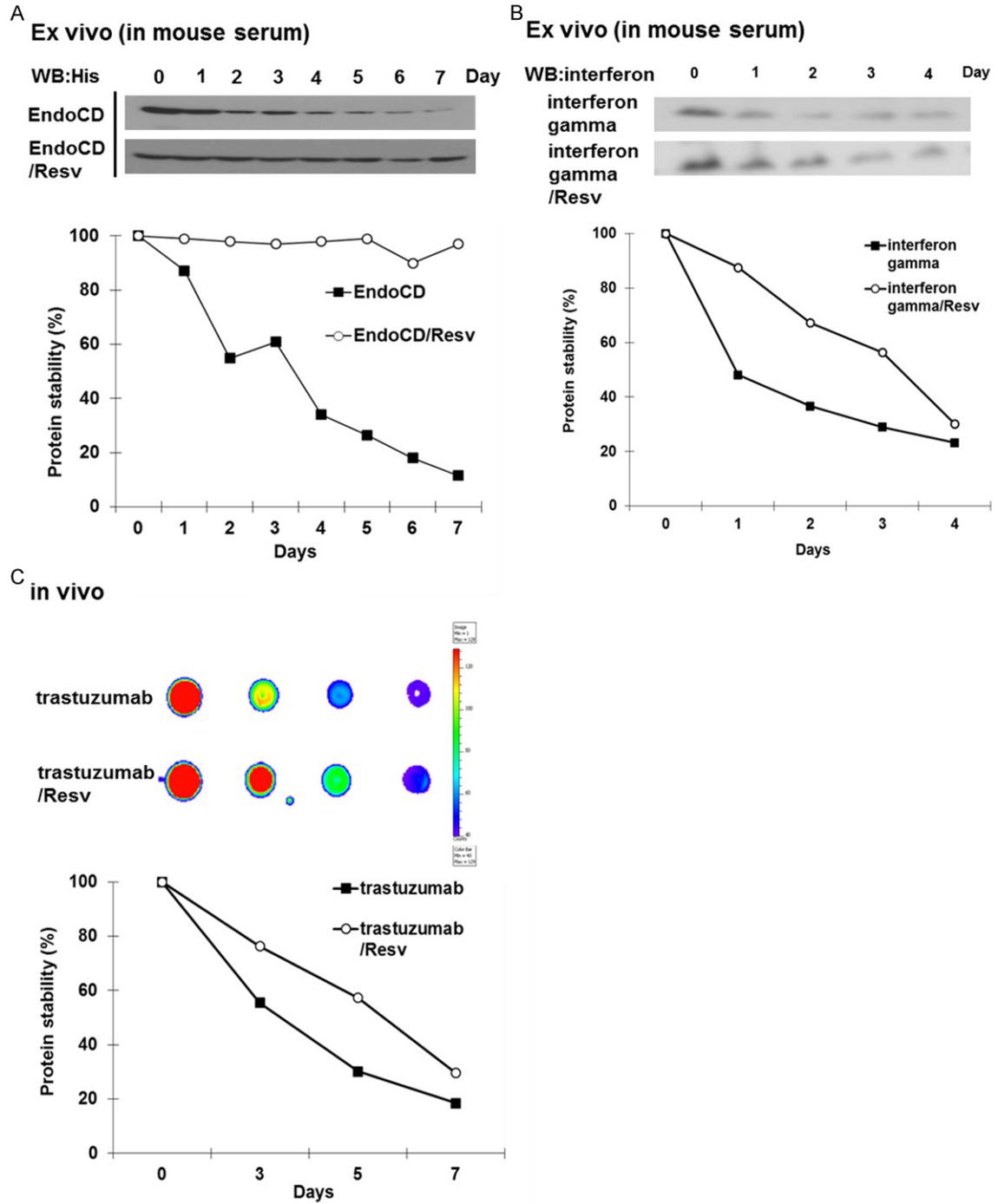
Figure S5. Resveratrol prolongs the protein stability of EndoCD fusion protein, INFγ, and trastuzumab. A. EndoCD protein (12.5 μM) or B. INFγ (2 μM) were mixed with mice sera with or without resveratrol, and at the indicated time points, an equal amount of protein was subjected to SDS-PAGE for Western blot analysis using anti-His-tag antibody or anti-INFγ gamma antibody. C. Mouse was administered trastuzumab (2 mg) by intravenous injection, and at the indicated time point mice serum was collected. An equal amount of serum was subjected to dot blot analysis for anti-human secondary antibody. Protein band and spot intensity was normalized to the intensity on day 0.
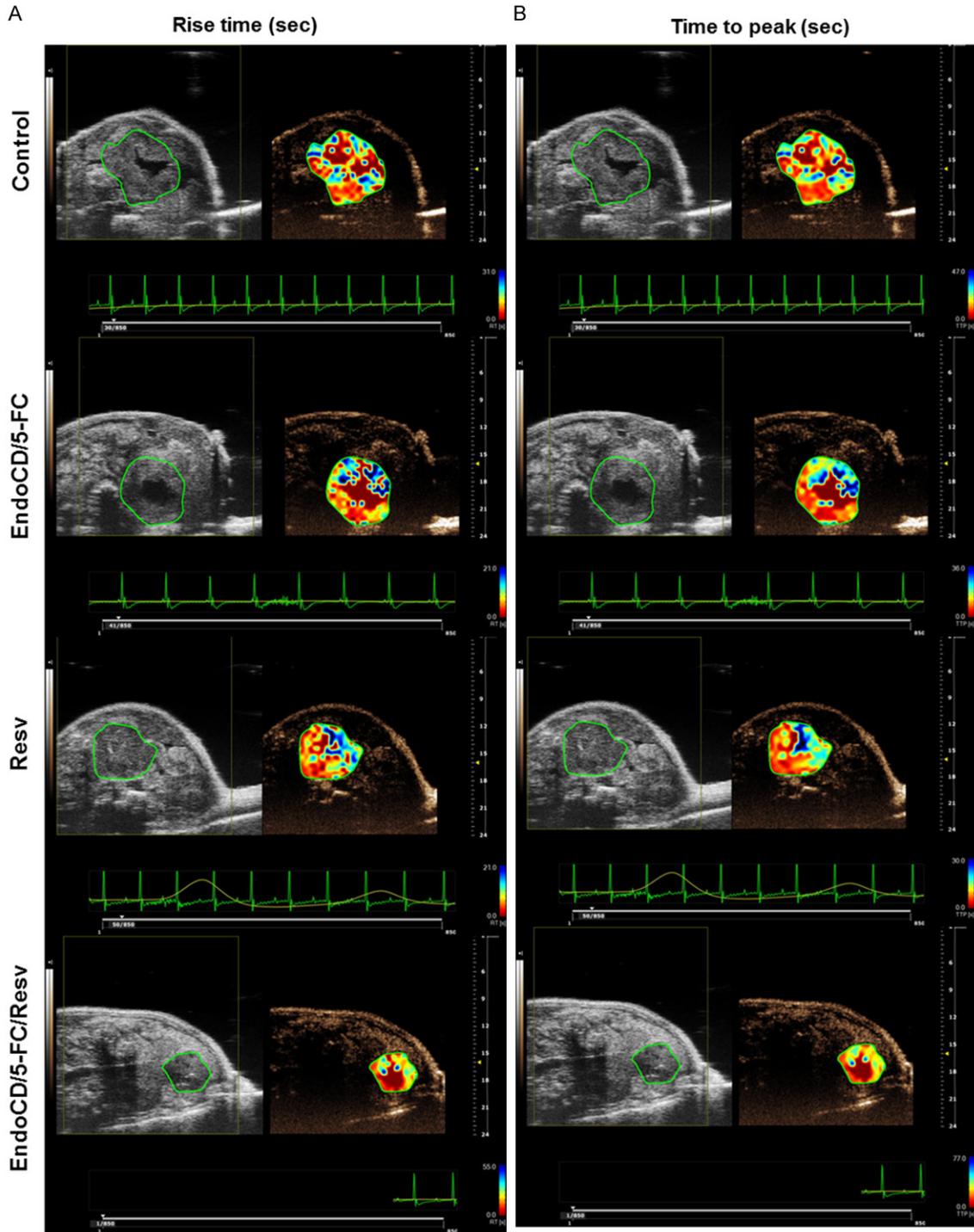
Figure S6. The effect of EndoCD/5-FC/resveratrol on stroma microenvironment by ultrasound imaging. Mice bearing stromal-enriched PDAC were treated with EndoCD/5-FC, resveratrol (Resv), or EndoCD/5-FC/Resv. Representative images showing blood flow parameters with the indicated treatment. A. Rise time. B. Time to peak. Quantitation is shown in **Figure 5A** to **5C**. *$P < 0.05$. 4 mice/group.
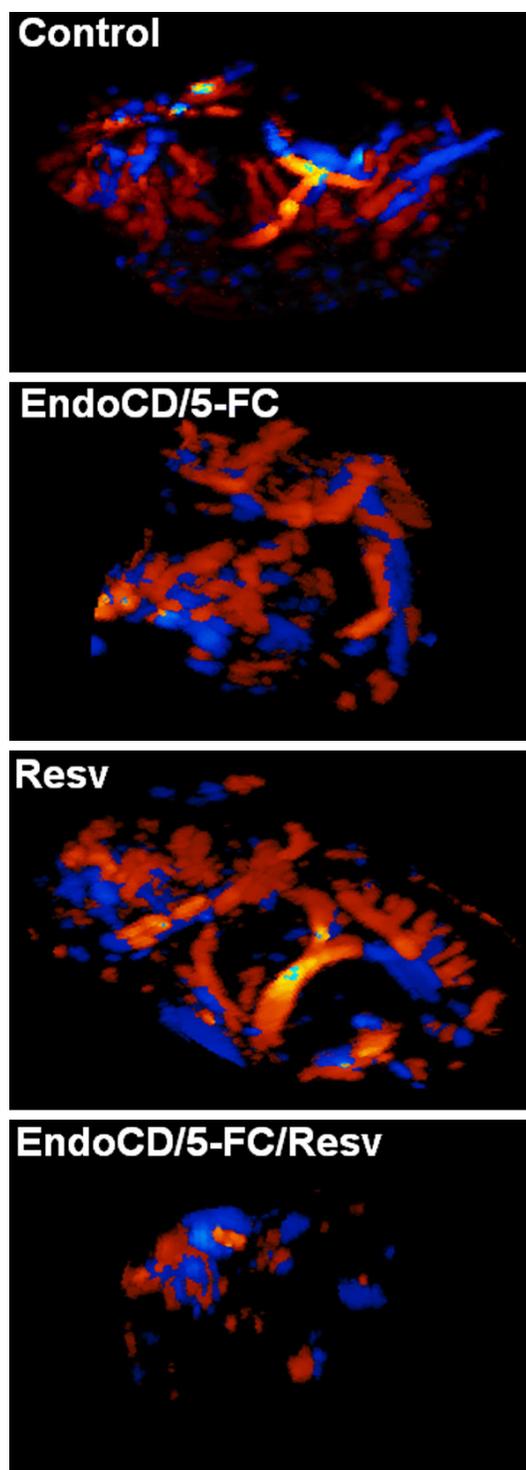
Figure S7. The effect of EndoCD/5-FC/resveratrol on stroma microenvironment by ultrasound imaging. Mice bearing stromal-enriched PDAC were treated with EndoCD/5-FC, resveratrol (Resv), or EndoCD/5-FC/Resv. Representative images of tumor vessel density with the indicated treatment. Quantitation is shown in **Figure 5D**. *$P < 0.05$. 4 mice/ group.
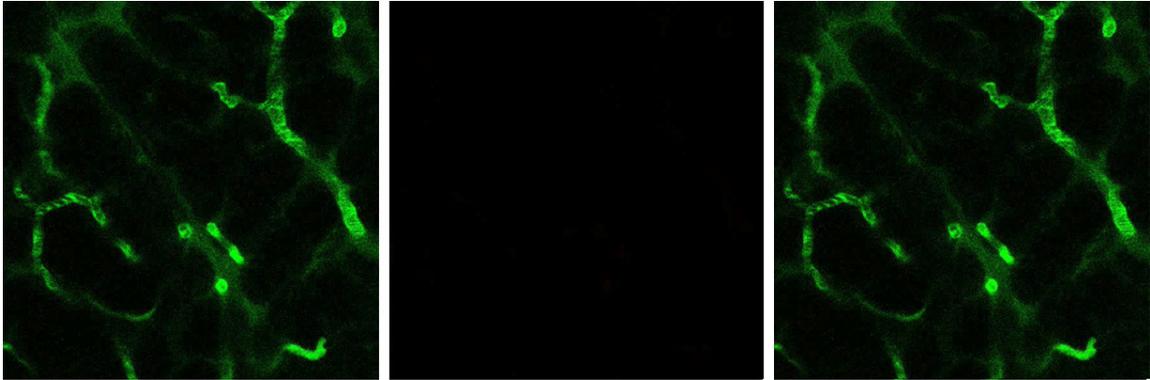
Movie S1. Time-lapse video of normal pancreatic vessels in mouse stromal-enriched PDAC model. Qdot605-labeled EndoCD was delivered systemically through mouse tail vein catheterization and monitored for its relative distribution. Vasculature was visualized by intravenously injection FITC-labeled dextran. Right panel movie shows FITC-labeled dextran. Middle panel movie shows Qdot605-labeled EndoCD. Left panel movie shows the merged images. Normal pancreas vessels were also recorded the Qdot605-labeled EndoCD signals after injection.
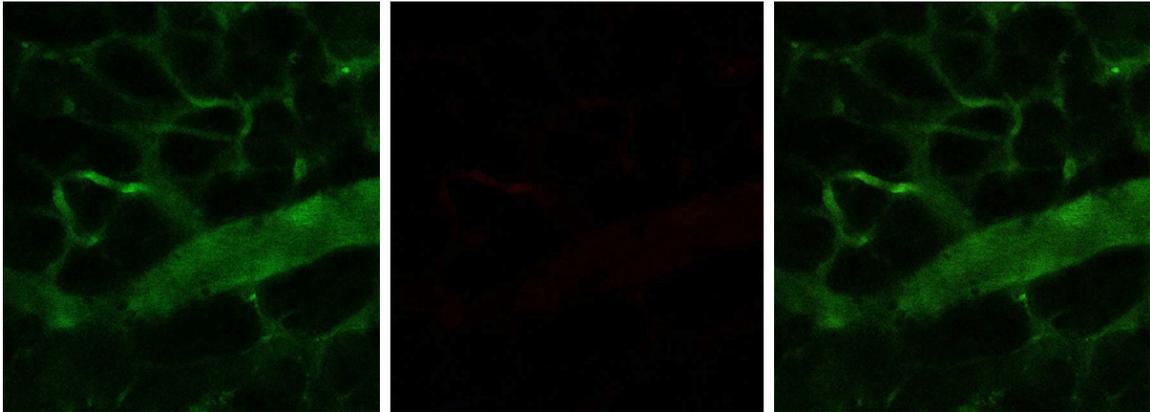
Movie S2. Time-lapse video of tumor pancreatic vessels in mouse stromal-enriched PDAC model. Qdot605-labeled EndoCD was delivered systemically through mouse tail vein catheterization and monitored for its relative distribution. Vasculature was visualized by intravenously injection FITC-labeled dextran. Right panel movie shows FITC-labeled dextran. Middle panel movie shows Qdot605-labeled EndoCD. Left panel movie shows the merged images.
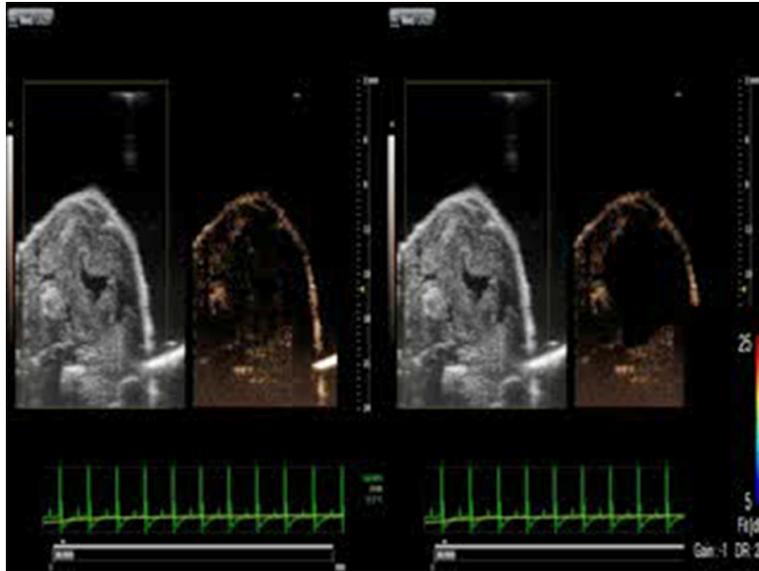
Movie S3. Time-lapse video of nonlinear contrast agent imaging of tumor blood blow in mice bearing stroma-enriched PDAC post control treatment. Contrast agent was injected into mice via tail vein catheterization and signals were recorded by ultrasound. Imaging was obtained using Contrast Mode on Vevo 2100 system. Left, before contrast agent injection. Right, after contrast agent injection.
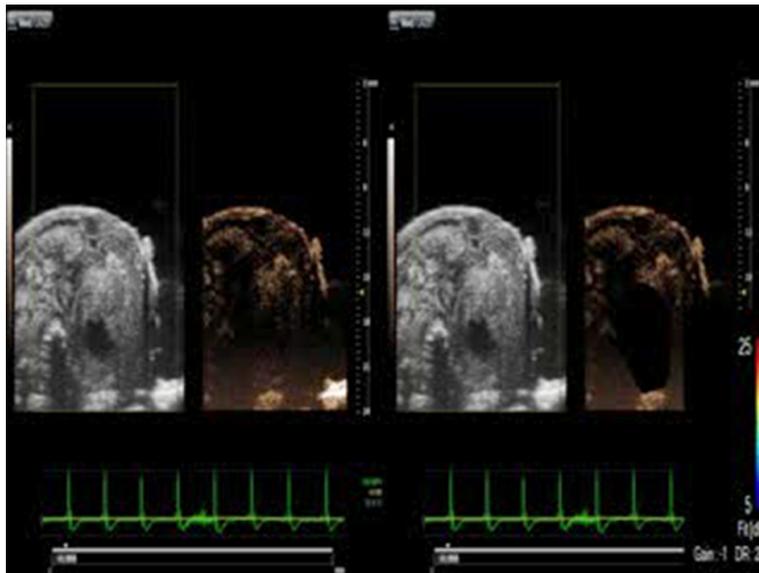
Movie S4. Time-lapse video of nonlinear contrast agent imaging of tumor blood blow in mice bearing stroma-enriched PDAC post EndoCD/5-FC treatment. Contrast agent was injected into mice via tail vein catheterization and signals were recorded by ultrasound. Imaging was obtained using Contrast Mode on Vevo 2100 system. Left, before contrast agent injection. Right, after contrast agent injection.
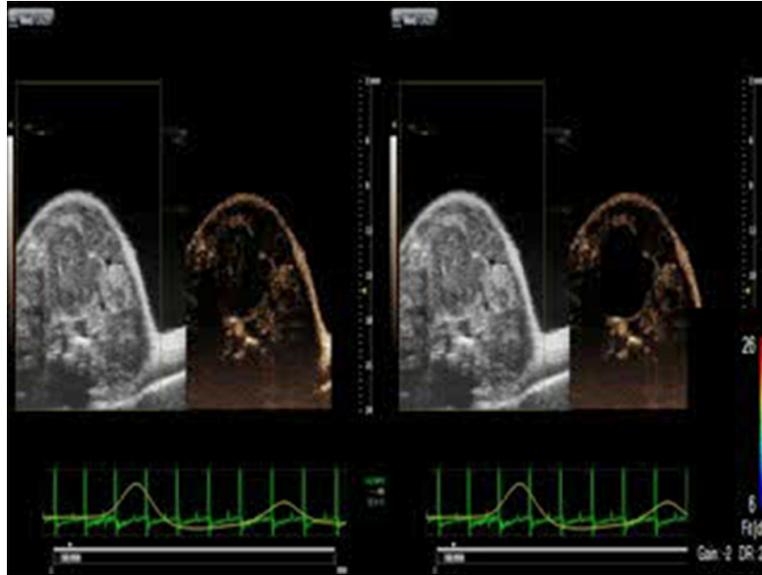
Movie S5. Time-lapse video of nonlinear contrast agent imaging of tumor blood blow in mice bearing stroma-enriched PDAC post resveratrol treatment. Contrast agent was injected into mice via tail vein catheterization and signals were recorded by ultrasound. Imaging was obtained using Contrast Mode on Vevo 2100 system. Left, before contrast agent injection. Right, after contrast agent injection.
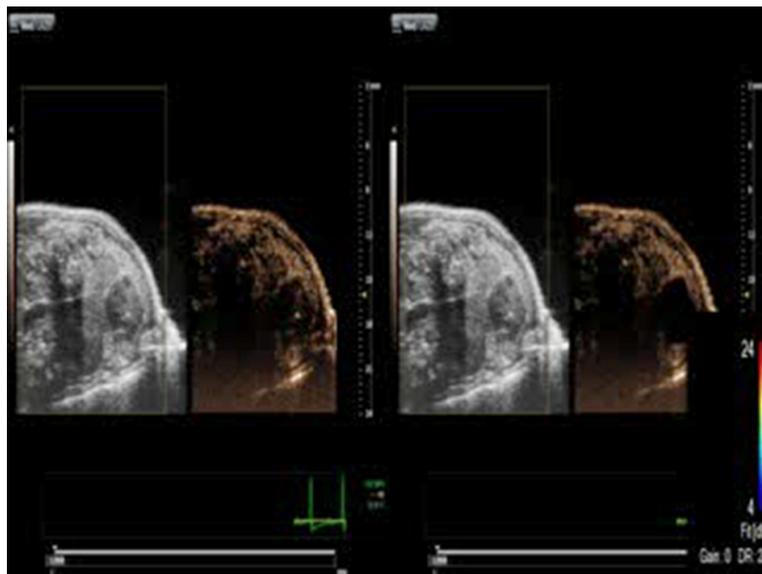
Movie S6. Time-lapse video of nonlinear contrast agent imaging of tumor blood blow in mice bearing stroma-enriched PDAC post EndoCD/5-FC/resveratrol treatment. Contrast agent was injected into mice via tail vein catheterization and signals were recorded by ultrasound. Imaging was obtained using Contrast Mode on Vevo 2100 system. Left, before contrast agent injection. Right, after contrast agent injection.